International Immunopharmacology 76 (2019) 105885

Contents lists available at ScienceDirect

International Immunopharmacology

journal homepage: www.elsevier.com/locate/intimp

p300 mediates the histone acetylation of *ORMDL3* to affect airway inflammation and remodeling in asthma

Qi Cheng*, Yunxiao Shang, Wanjie Huang, Qinzhen Zhang, Xiang Li, Qianlan Zhou

Pediatric Pulmonology Department, Shengjing Hospital of China Medical University, 36th Sanhao Street, Heping District, Shenyang 110004, PR China

ARTICLE INFO

Keywords:
Asthma
ORMDL3
p300
Histone acetylation

ABSTRACT

Background: Bronchial asthma is affected by both environmental and genetic factors. The orosomucoid 1-like protein 3 (*ORMDL3*) gene is related to childhood asthma and is involved in airway inflammation and airway remodeling. The *ORMDL3* promoter contains binding sites for the histone acetylase p300. Gene expression can be affected by epigenetic modifications. This study aimed to investigate whether the p300-mediated histone acetylation (HAT) of *ORMDL3* gene affects airway inflammation and remodeling in asthma.

Methods: 16HBE14o- cells were transfected with various concentrations of a wild-type p300 plasmid or p300HAT-deletion plasmids. A dual luciferase reporter assay was used to examine the effect of p300-mediated HAT on the *ORMDL3* promoter. Thirty BALB/c mice were randomly divided into a control group, an ovalbumin (OVA)-induced asthma group and an asthma + C646 (a selective inhibitor of p300) group. Noninvasive lung function tests were conducted to examine airway hyperreactivity (AHR) in the different groups. HE and Masson's trichrome staining was performed to examine airway remodeling and inflammation. Immunohistochemistry, western blotting and real-time PCR were used to analyze *ORMDL3* expression in lung tissues. ELISA and western blotting were used to evaluate the HAT status in lung tissue. The ChIP assay was used to determine the relationship of the *ORMDL3* promoter to p300 or acetylated histone H3 (aceH3).

Results: p300 activated transcription from the *ORMDL3* promoter, resulting in an increase in endogenous *ORMDL3* mRNA levels. *ORMDL3* promoter activity was reduced when the HAT activity of p300 was lost. *ORMDL3* expression was elevated, and HAT activity was high in the lung tissues of asthmatic mice. p300 and aceH3 bound to the promoter region of *ORMDL3*. In the asthma group, the amounts of p300 and aceH3 recruited to the *ORMDL3* promoter were increased. C646 inhibited p300 expression and reduced HAT activity and aceH3 levels in asthmatic mice, thereby reducing *ORMDL3* expression and relieving AHR and airway remodeling.

Conclusion: p300-mediated HAT modulates the expression of the asthma susceptibility gene *ORMDL3*, thereby improving the process of airway inflammation and remodeling in asthma.

1. Introduction

Bronchial asthma is the most common chronic nonspecific inflammatory airway disease in children. The incidence of bronchial asthma has increased significantly in recent years. Epidemiological studies show that asthma is affected by both genetic and environmental factors and that it is characterized by chronic airway inflammation, airway hyperreactivity (AHR) and irreversible airway remodeling. Discovered in 2007 by Moffatt et al. [1], the orosomucoid 1-like protein 3 (*ORMDL3*) gene is located on chromosome 17q21. To date, *ORMDL3* is the gene most strongly linked to childhood asthma [2]. The correlation between *ORMDL3* and asthma has been demonstrated in a variety of ethnic groups [3]. Elevated *ORMDL3* expression is detected in more than one third of asthmatic children < 7 years of age. We previously found that *ORMDL3* affects airway inflammation and remodeling in asthma and induces bronchial epithelial-mesenchymal transition (EMT) [4]. Therefore, inhibition of *ORMDL3* overexpression and exploration of the mechanisms underlying the regulation of *ORMDL3* may help identify new targets for the treatment of asthma.

Some scholars have proposed the gene-environment interaction hypothesis. This hypothesis holds that the functions of many known genes are determined by environmental factors and that epigenetic modification is an important mechanism underlying the interplay between environmental and genetic factors [2,5]. Moheimani et al. have found that the interaction between genes and epigenetic modifications induces changes in the structure and function of the airway epithelium

* Corresponding author at: Pediatric Pulmonology Department, Shengjing Hospital of China Medical University, Shenyang 110004, PR China.
E-mail address: silvia.cq@163.com (Q. Cheng).

https://doi.org/10.1016/j.intimp.2019.105885
Received 15 May 2019; Received in revised form 20 August 2019; Accepted 5 September 2019
1567-5769/ © 2019 Published by Elsevier B.V.

and contributes to the pathogenesis of asthma [6]. Histone acetylation is one of the most common epigenetic modifications. DNA is wound around the histone octamer. Acetylation (a covalent modification) of the N-terminal region of histones regulates DNA transcription and contributes to the regulation of gene expression [7]. Barnes et al. found that the levels of histone acetyltransferases (HATs; p300 and CBP) were significantly increased and that the levels of histone deacetylases (HDACs) were decreased in bronchial biopsy specimens of asthmatic patients compared with healthy individuals; these changes are conducive to the release of inflammatory factors that play important roles in the amplification and maintenance of inflammatory responses and represent the molecular mechanism underlying chronic inflammation and airway remodeling [8–10].

Studies have found that the promoter region of *ORMDL3* contains binding sites for p300 HAT. p300 facilitates the binding of transcription factors such as ETS-1 and signal transducer and activator of transcription 6 (STAT6) to the *ORMDL3* promoter; this binding is necessary for the maintenance of the basic transcriptional activity of *ORMDL3* gene [11,12]. p300 is a classic endogenous HAT [13]; it is highly conserved among organisms and plays important roles in cell cycle maintenance, cell transformation and apoptosis. To date, three primary biological functions of p300 have been discovered. (1) p300 acts as a HAT by acetylating the N-terminus of histone; this modification results in an open chromatin structure and facilitates transcription. (2) As an acetylase, p300 acetylates nonhistone transcription factors, thereby enhancing their activity. (3) p300 functions as a transcriptional activator; it recruits transcription factors to the promoter regions of target genes, thereby facilitating transcription.

Therefore, whether *ORMDL3* overexpression in asthma is regulated by p300-mediated histone acetylation is worthy of investigation. In the present study, we evaluated the importance of p300-mediated histone acetylation in the regulation of *ORMDL3* gene expression *in vitro*. Subsequently, we investigated the expression and relationship among *ORMDL3* and p300 and histone acetylation in the lung tissues of asthmatic mice. Finally, the effects of C646 (a selective inhibitor of p300 [14]) on histone acetylation, *ORMDL3* expression, airway inflammation, airway remodeling and airway responsiveness were evaluated *in vivo*.

2. Methods

2.1. Animal model and ethical approval

A total of 30 specific-pathogen-free female BALB/c mice (8 weeks old) were purchased from the experimental animal research center of Shengjing Hospital of China Medical University (Shenyang, China). All experimental protocols involving animals were approved by the research ethics committee of China Medical University and complied with the guidelines set forth by the China Council on Animal Care. The animals were randomly assigned to three groups: a model group (n = 10); a control group (n = 10); and a C646 group (n = 10). The mice in the model group were treated according to previously described methods with a modified ovalbumin (OVA) (Sigma-Aldrich, Beijing, China) immunization protocol that was developed to induce allergic asthma in mice [10]. The mice were initially intraperitoneally immunized with 20 μg of OVA and 2 mg of aluminum hydroxide gel (Sigma-Aldrich, Beijing, China) in 0.5 ml of PBS on days 0, 7, and 14 as previously reported [4]. The control mice received intraperitoneal injections of saline alone. From day 16 onwards, the animals were treated every other day for 14 days as follows. The mice in the model group were placed in a transparent glass chamber (approximately 20 cm × 20 cm × 20 cm in volume) connected to an ultrasonic nebulizer (Model 100, Yadu, Shanghai, China) and subjected to repeated bronchial allergen challenge by inhalation of OVA (4%) for 30 min/day. The mice in the C646 group were intraperitoneally injected with 10 μg of C646 in 0.5 ml of PBS prior to OVA challenge. The lung function of the mice in all groups was evaluated on the last day of OVA challenge; the mice were then anesthetized by intraperitoneal injection of 5% chloral hydrate and sacrificed. The lungs of the mice were collected aseptically by chest opening. The left lung of each animal was fixed in paraformaldehyde (PFA) for subsequent IHC staining; the right upper lung lobes were used for ChIP and real-time PCR analysis, and the right lower lung lobes were used for western blots. All specimens were snap-frozen in liquid nitrogen and stored at −80 °C until use.

2.2. Measurement of airway high reactivity (AHR)

AHR measurement was performed by whole-body plethysmography (Buxco, Troy, NY, USA). The pressure differences between the main chamber of the plethysmograph, which housed the animal, and a reference chamber (box pressure signal) were measured. The mice were challenged with aerosolized normal saline (for the baseline measurement) or methacholine (3.125, 6.25, 12.5, 25 and 50 mg/ml) for 3 min, and readings were obtained and averaged for 3 min after nebulization. The results are expressed as the percent increase in the enhanced pause (Penh) value after challenge with each increasing concentration of methacholine.

2.3. Bronchoalveolar lavage (BAL) and counting cells

Following the measurement of lung responsiveness, the mice were sacrificed with an overdose of chloral hydrate. A catheter was inserted into the trachea, and BAL was performed using three aliquots of 0.5 ml of PBS (pH 7.2) and withdrawn three times each. The qualified fluid recovery rate was over 80%. The cell suspension was concentrated by centrifugation (1000 rpm, 10 min at 4 °C), and the cell pellet was resuspended in a 1-ml saline solution. To perform the differential leukocyte cell count, 0.1 ml of the cell suspension was dropped on a glass slide and stained with a Wright–Giemsa stain. A microscope was then used to examine 200 nucleated cells.

2.4. Lung histopathology

The left lung of each animal was fixed in 4% PFA for 18–24 h, embedded in paraffin and routinely processed. Serial 5-μm tissue sections were stained with HE for general histological evaluation. Masson's trichrome staining was performed for the assessment of collagen particles and airway remodeling.

2.5. Morphometric analysis of the airway

HE- and MT-stained tissue sections were examined by light microscopy at a magnification of 200×. To assess bronchiolar remodeling and collagen deposition, morphometric measurements were obtained using Image-Pro Plus 6.0 software. In HE-stained lung sections from each group, complete cross-sections of the bronchiole without cartilage were selected for analysis. The total bronchial wall area (Wat, μm^2) and the diameter of the basal membrane perimeter (Pbm, μm) were analyzed for each bronchiole. Wat/Pbm expresses the wall thickness of the bronchiole wall. MT staining was used to assess collagen deposition. Two complete bronchioles were selected from each tissue section, and the percentage of the total stained area showing collagen deposition was calculated [15,16].

2.6. Immunohistochemistry

ORMDL3 protein expression in the lung was detected by immunohistochemistry. Lung sections of 5 μm were cut and blocked with peroxide and nonimmune animal serum and incubated sequentially with primary antibody (rabbit polyclonal anti-*ORMDL3* LifeSpan BioSciences 1:200), biotin-labeled secondary antibody, and streptomycin anti-biotin peroxidase. Finally, the sections were stained with

DAB, counterstained with hematoxylin, dehydrated, cleared in xylene, and fixed. Negative staining controls were generated by replacing the primary antibody with PBS. A laser scanning confocal microscope (MTC-600, Bio-Rad, Hercules, CA, USA) was used for image acquisition, and the deposition of brown particles in the cytoplasm indicated a positive result.

2.7. Western blot analysis

Total protein extracted from lung tissue and 16HBE14o- cells was quantified using a BCA protein assay kit. Protein samples (20 μl) were then separated on 12% SDS-PAGE gels and transferred to polyvinylidene difluoride membranes (Millipore, Billerica, MA, USA). The membranes were blocked with 5% skim milk for 1 h and then incubated with primary antibodies (*ORMDL3* 1:800; p300 1:100; aceH3 1:4000; GAPDH 1:200) diluted in PBS overnight at 4 °C. After washing in Tris-buffered saline containing 1% Tween-20 (TBST), the membranes were incubated for 2 h with a horseradish peroxidase-conjugated secondary antibody (1:500) and imaged using enhanced chemiluminescence reagents. The density of the protein bands was analyzed using ImageJ software. GAPDH was used as an internal control.

2.8. Real-time PCR

Total RNA was isolated according to the manufacturer's instructions using TRIzol reagent (Invitrogen, Carlsbad, CA, USA) and RNAiso™ Plus reagent (Takara, Dalian, China) and quantified using a spectrophotometer. Following quantification, 2 μg of RNA was reverse-transcribed into cDNA, and real-time quantitative PCR assays were conducted using an ABI PRISM 7500 Real-time PCR System (Applied Biosystems, Foster City, CA, USA) and SYBR PrimeScript™ RT-PCR kit reagent (Takara, Dalian, China). The PCR conditions for NK-1R were 40 cycles of denaturation at 95 °C for 5 s and annealing and extension at 60 °C for 30 s. Target mRNA levels were normalized to those of GAPDH. The oligonucleotide primers used are presented in Table I.

2.9. Chromatin immunoprecipitation (ChIP) assay

ChIP was performed using an EZ-ChIP kit (Millipore) according to the manufacturer's instructions. In brief, lung tissues obtained from animals in the model and control groups at 14 days were treated with formaldehyde (1% final concentration); after protein-DNA crosslinking, genomic DNA was ultrasonically sheared to lengths of 200–1000 bp. Nonspecifically binding proteins and DNA were removed using Protein G agarose, and an antibody-free control sample was set aside. Normal mouse IgG (IgG group), anti-aceH3 (1:500, Millipore) or anti-p300 (1:500, Santa Cruz) and Protein G agarose were then added, and the samples were incubated overnight. The samples were washed according to instructions provided with the kit, eluted with elution buffer to remove protein/DNA complexes, cross-linked, subjected to stepwise purification, and amplified. The amplification conditions were the same as those used for real-time PCR; the primer sequences are shown in Table 1. The model results are expressed as 2-CT (Target gene group-Input group IgG group).

2.10. HAT activity assay of lung tissue

Nuclear proteins were extracted from lung tissue using the Nuclear Extract Kit (KeyGEN BioTECH, Jiangsu, China) according to the manufacturer's instructions. The HAT activity of the nuclear protein extract was determined by a colorimetric method using a HAT assay kit (k332, BioVision, Mountain View, CA, USA). The ELISA plates were precoated with 100 μl of 1 μg/ml reconstituted histone H3 and incubated overnight at 4 °C. The nuclear extract (50 μg) was incubated with the HAT reaction cocktail in a 96-well plate at room temperature for 4 h; HAT assays were then performed according to the manufacturer's instructions. The plates were read on an enzyme microplate reader (Thermo Scientific, New York, USA) at a wavelength of 440 nm. Each assay group was measured in triplicate.

2.11. Plasmids

pcDNA3.1-p300 and pcDNA3.1-p300 (HAT-) (Addgene plasmids 23252 and 23254, gifts from Warner Greene) were prepared by subcloning the p300 and p300AT2Mut fragments from pBS-p300 and pBS-p300 AT2 Mut [17] into the *Hin*dIII and *Not*I sites of the pcDNA3.1 vector (V79520, Invitrogen, USA) [18]. pcDNA3.1-p300 was for the wild type p300 plasmid (p300 WT); pcDNA3.1-p300 (HAT-) was for the p300 (HAT-) plasmid. The DNA sequence −1812/−922 of the human *ORMDL3* gene promoter region was amplified by PCR. The resulting fragment was cloned into the pUM-T simple vector (BioTeke, Beijing, China) digested with Fast Digest *Nhe* I and Fast Digest Hind III and subcloned into the promoterless luciferase expression plasmid pGL3-Basic (Promega, Beijing, China) to create the *ORMDL3* promoter/luciferase plasmid pGL3-P-Luc.

2.12. Cell transfection and luciferase assays

Immortalized SV-40 virus-transformed human bronchial epithelial cells (16HBE14o-) were purchased from the cell line resource of XiangYa School of Medicine. 16HBE14o- cells were efficiently co-transfected either varying amounts (0.25 μg, 0.5 μg, 1 μg, 2 μg, and 4 μg) of p300WT or p300 (HAT-) plasmid together with 1 μg of the promoter reporter plasmids and 10 ng of the pRL-TK plasmid using Lipofectamine 2000 (Invitrogen, USA) according to the manufacturer's instructions. Cells were cotransfected with 1 μg of the promoter reporter plasmids together with 10 ng of the pRL-TK plasmid (Promega, Beijing, China) as an internal control. The cells were harvested 24 h after cotransfection, and western blotting and real-time PCR assays were conducted. Luciferase activity was measured using the Dual Reporter Assay System (E1910, Promega, USA) and a spectrofluorometer (Lumat LB9507, Berthold, Germany). The results shown are representative of at least three independent experiments performed in triplicate.

Table 1
Sequences of primers used for real-time PCR.

Gene name	Species	Forward primer	Reverse primer
GAPDH	Human	GAGAAGGCTGGGGCTCATTT	AGTGATGGCATGGACTGTGG
ORMDL3promotor	Human	GGACTGCTAGCTCCTGCATAGAGTGGACTTA	GCTCTAAGCTTGGTTGGAAGTTGTACCGTGA
p300	Human	GGGACTCAGCACCGATAACTCA	ACTGCACAGTTCTTATGTGTTCCAA
ORMDL3	Human	GAGCATCCCGTTTGTGAGTGTC	CCATCTGCTCCCAGTGGGTTA
GAPDH	Mouse	CTACCCCCAATGTGTCCGTC	GGGATAGGGCCTCTCTTGCT
ORMDL3	Mouse	CCCTGTGGGTTTGAACTCCTG	GTCGAAGTGAACCCGCTTCTG
p300	Mouse	TTCAGCCAAGCGGCCTAAAC	GTTCCAGGTCAAACAGTGAACCAA
ORMDL3promotor	Mouse	TCAGGGTGGGACGTTCTGCG	CGTTGTGCCTCTTGGGAAGTGTAGTT

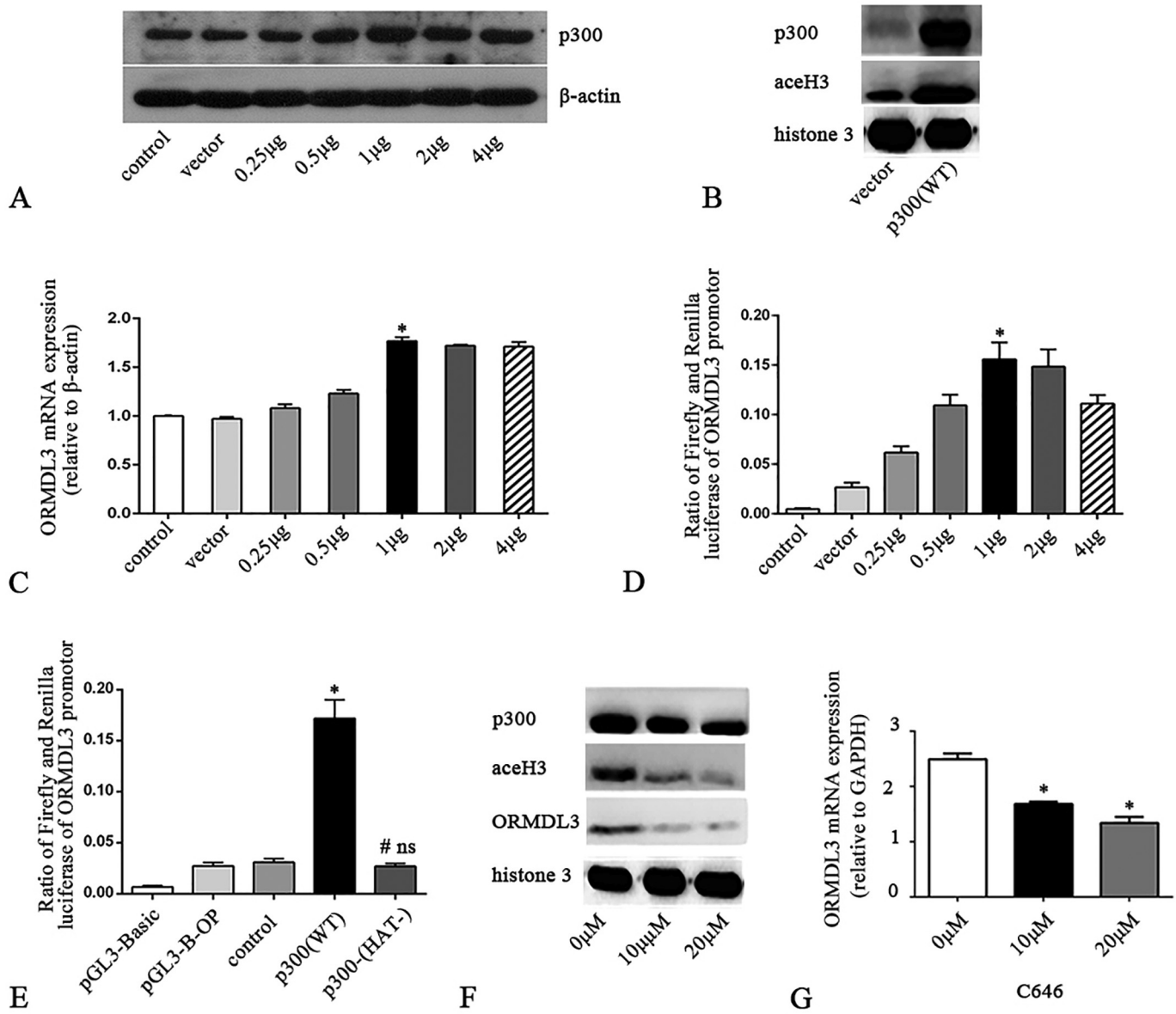

Fig. 1. *ORMDL3* expression after p300 transfection of 16HBE14o- cells *in vitro*. Western blot showing the level of expression of p300 protein after transfection of the cells with increasing amounts (0.25, 0.5, 1, 2 or 4 μg) of the p300WT plasmid; p300 protein expression reached a peak level when the cells were transfected with 1 μg of p300 plasmid (A). Acetylation level of histone3 increased when the cells were transfected with 1 μg of p300 plasmid, as shown by western blot (B). Real-time PCR results indicate the expression of endogenous *ORMDL3* mRNA (C) *, $p < 0.01$. The activity of the *ORMDL3* promoter after transfection of cells with various concentrations of p300WT plasmid was tested using a dual luciferase assay (D) *, $p < 0.01$. A dual luciferase assay was used to compare the activity of the *ORMDL3* promoter after transfection of the p300 WT plasmid and the p300 (HAT-) mutant plasmid into 16HBE14o- cells (E). Different doses of C646 (0 μg, 10 μg, 20 μg) were added to the cells; the protein levels of p300, aceH3 and *ORMDL3* were detected by western blot (F), and the mRNA level of *ORMDL3* was detected by real-time PCR (G). *, control *vs.* p300(WT), $p < 0.01$; #, p300(WT) *vs.* p300 (HAT-), $p < 0.01$; ns, control *vs.* p300 (HAT-).

2.13. Statistical analysis

The data were evaluated using one-way analysis of variance (ANOVA) followed by Bonferroni's multiple comparison test using the GraphPad Prism software; $p < 0.05$ was considered significant. The data are presented as x ± sd (mean ± standard deviation). Statistical analysis was performed using SPSS23.0 software.

3. Results

3.1. p300 transfection induced histone 3 acetylation and enhanced ORMDL3 mRNA expression

To demonstrate that p300 can induce the acetylation of histone 3 and regulate *ORMDL3* expression, 16HBE14o- cells were transfected with varying amounts of p300WT plasmid (0.25, 0.5, 1, 2 and 4 μg) or empty pcDNA3.1 vector. p300 protein expression reached a peak level when the cells were transfected with 1 μg of p300 plasmid; that is, transfection reached saturation when 1 μg of p300 plasmid was added to the cells (Fig. 1A). p300 overexpression led to histone acetylation (Fig. 1B) and enhanced *ORMDL3* expression (Fig. 1C).

A positive correlation was observed between the amount of p300WT plasmid used in the transfection and the endogenous *ORMDL3* mRNA level. The correlation coefficient was 0.939 ($p < 0.01$, Fig. 1C).

3.2. p300 activated ORMDL3 promoter in a dose-dependent manner

16HBE14o- cells were cotransfected with the p300WT plasmid

(0.25, 0.5, 1, 2 or 4 μg), 1 μg of the *ORMDL3* promoter plasmid and 10 ng of the pRL-TK plasmid. These plasmids constituted the luciferase reporter system. As shown in Fig. 1D, the *ORMDL3* promoter activity (expressed as fluorescence intensity) changed as the amount of the p300WT plasmid used in the transfection changed. The correlation coefficient was 0.956 ($p < 0.01$). The *ORMDL3* promoter exhibited maximum activity when the cells were transfected with 1 μg of p300WT plasmid. That is, the *ORMDL3* promoter was activated by p300 transcription.

3.3. The HAT activity of p300 was necessary for ORMDL3 transcription

16HBE14o- cells were transfected with the p300WT plasmid or the p300HAT-mutant plasmid. Fluorescence intensity was significantly decreased ($p < 0.01$) in the p300HAT- group compared with cells transfected with the p300WT plasmid. The p300HAT- group did not show a significant difference in fluorescence intensity compared with the pGL3-B-OP group or the p300 empty vector group ($p > 0.05$). These results demonstrate that the HAT activity of p300 was required for transcription driven by the *ORMDL3* promoter (Fig. 1E).

3.4. The effect of C646 on p300 and acetylation of histone 3 and ORMDL3 in vitro

To determine the effect of the specific histone acetylase p300 inhibitor C646 on p300 and the acetylation of histone 3 and *ORMDL3,* different doses of C646 (0 μg, 10 μg, 20 μg) were added to 16HBE14o- cells. The results indicated that C646 had no significant effect on the expression of p300 protein but significantly reduced the acetylation level of histone 3 and negatively affected the expression of *ORMDL3* protein and mRNA (Fig. 1F, G).

3.5. ORMDL3 expression level in asthmatic lung tissues

ORMDL3 expression in asthmatic lung tissue was examined by immunohistochemistry (IHC), western blotting and real-time PCR. Strong *ORMDL3* staining was observed in the bronchial epithelium and in perivascular infiltrating cells in the OVA-induced asthmatic mice. In contrast, mice from the control group showed faint *ORMDL3* staining, observed only at a low level around the blood vessels (Fig. 2A). Western blotting and real-time PCR showed that *ORMDL3* protein and mRNA expression were significantly increased in the OVA-induced asthma group compared with the control group (Fig. 2B, C).

3.6. Histone acetylation was increased in asthmatic lung tissues

To explore the mechanism of action of histone acetylation in asthma, we first evaluated histone acetylation levels in lung tissues by examining HAT activity and p300 and aceH3 levels in lung tissues.

HAT activity was significantly elevated in the OVA-induced asthma group compared with the control group through ELISA ($p < 0.01$, Fig. 3A). Western blotting was performed to examine aceH3 levels in lung tissues. aceH3 expression was significantly higher in the OVA-induced asthma group than in the control group ($p < 0.01$, Fig. 3B).

Western blotting and real-time PCR showed that p300 protein and mRNA levels were significantly increased in the OVA-induced asthma group compared with the control group (Fig. 3C, D).

3.7. p300 and aceH3 bound to the promoter region of the ORMDL3 gene and affected ORMDL3 expression in asthmatic lung tissues

ChIP assays were performed to determine whether p300 and aceH3 bind to the promoter region of the *ORMDL3* gene in lung tissues. In addition, the effect of asthma on p300 and aceH3 binding was investigated. The chromatin precipitated with aceH3 and p300 antibodies was analyzed by real-time PCR to determine the quantity of *ORMDL3* gene promoter fragments present in the immunoprecipitate. It was found that the amount of *ORMDL3* recruited by aceH3 and p300 was significantly higher in the OVA-induced asthma group than in the control group ($p < 0.01$, Fig. 4A, B). A portion of the ultrasonically fragmented chromatin was used as an input control and compared with the amplification products of real-time PCR. The results were verified by agarose gel electrophoresis. In addition, the efficiency of ChIP was determined. The results of these additional experiments verified that the amount of *ORMDL3* recruited by aceH3 and P300 was significantly higher in the OVA-induced asthma group than in the control group (Fig. 4C, D).

3.8. The effect of C646 on acetylation of histone 3, ORMDL3, airway reactivity and airway remodeling in asthmatic mice

When the mouse model of asthma had been successfully established, the mice were intraperitoneally injected with C646, and the resulting changes in histone acetylation in their lung tissues were examined. Compared with the OVA-induced asthma group and the control group, the C646 group exhibited reduced HAT activity ($p < 0.01$, Fig. 3A). aceH3 levels and p300 protein and mRNA levels were decreased in the C646 group compared with the asthma group ($p < 0.01$). However, there were no significant differences between the C646 group and the control group in the levels of p300 ($p > 0.05$, Fig. 3B, C, D). The amount of *ORMDL3* recruited by p300 and aceH3 was markedly reduced in the C646 group compared with the OVA-induced asthma group ($p < 0.01$). Again, there was no significant difference in the amount of recruited *ORMDL3* between the C646 group and the control group ($p > 0.05$, Fig. 4). Compared with the OVA-induced asthma group, the lung tissues of mice in the C646 group displayed reduced *ORMDL3* protein and mRNA content ($p < 0.01$). However, no significant differences were found in *ORMDL3* protein or mRNA levels between the C646 group and the control group ($p > 0.05$, Fig. 2). The above results indicate that C646 not only inhibited histone acetylation in asthmatic lung tissues but also suppressed *ORMDL3* expression through the regulation of p300 and acetyl H3.

ORMDL3 is one of most importance susceptibility genes of asthma. The present study investigated whether C646 inhibited asthma processes, including AHR, airway inflammation and remodeling. Lung function tests showed that airway resistance was reduced in the C646 group compared with the OVA-induced asthma group upon ACH challenge ($p < 0.01$, Fig. 5G). The total number of leukocytes and eosinophils was decreased in C646 group compared with the OVA-induced asthma group. The Wat/Pbm ratio and the percentage area of collagen deposition were decreased in the C646 group compared with the OVA-induced asthma group ($p < 0.01$, Fig. 5A-F). Thus, inhibition of HAT reduced AHR and the extent of airway remodeling in asthmatic mice.

4. Discussion

The possibility that *ORMDL3* is closely related to asthma has been confirmed in multiple ethnic groups and in numerous epidemiological studies. *ORMDL3* is considered to be a susceptibility gene that is most closely related to asthma. The *ORMDL3* gene is a member of the ORM gene family, which includes ORMDL1, ORMDL2, and *ORMDL3*. The *ORMDL3* gene is located on chromosome 17q21 and encodes a 153-amino acid tetraspan transmembrane protein that is anchored in the endoplasmic reticulum (ER). *ORMDL3* is widely expressed in human tissues. In particular, high levels of *ORMDL3* expression have been detected in the liver and in peripheral blood lymphocytes [19]. Our previous study found that *ORMDL3* expression was increased in bronchial epithelial cells and perivascular inflammatory cells in asthmatic mice. In contrast, *ORMDL3* is rarely expressed in the bronchial epithelial cells of normal controls [4]. *ORMDL3* is anchored to the ER and colocalizes with the calcium pump. *ORMDL3* affects calcium ion balance and promotes ER stress and the unfolded protein response by

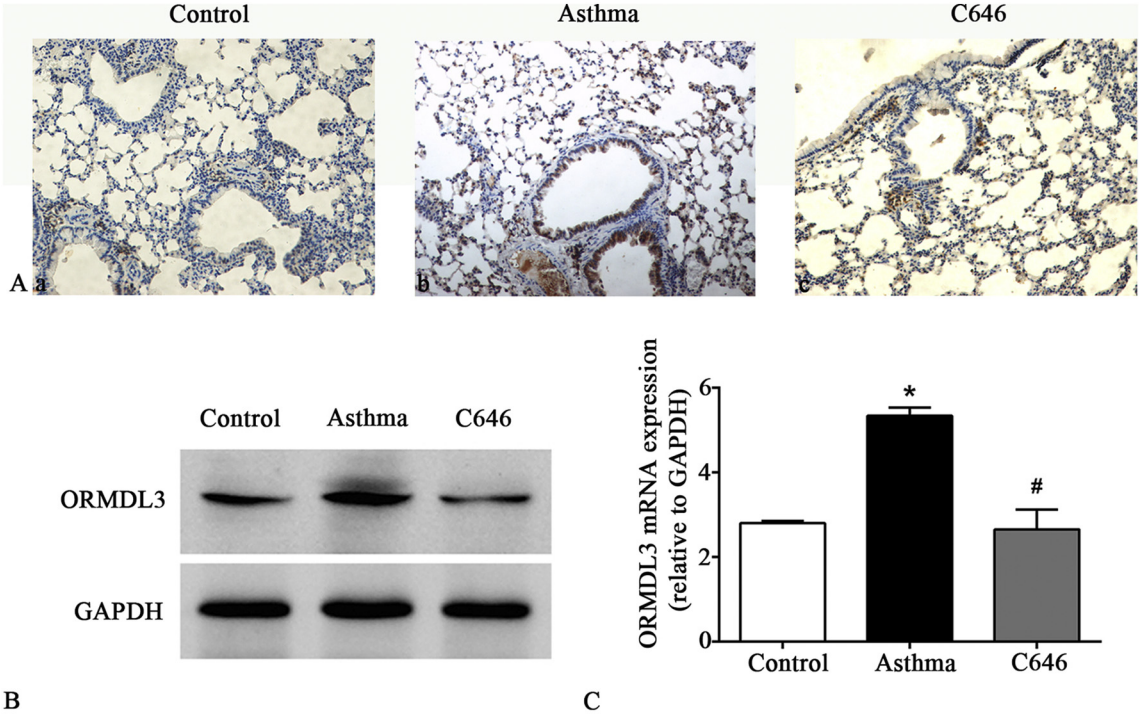

Fig. 2. *ORMDL3* expression in the lung tissue of mice. *ORMDL3* IHC (200×) of paraffin sections of lung tissue from BALB/c mice in the control group (A a), the asthma group (A b), and the C646 group (A c). The expression of *ORMDL3* protein and mRNA in lung tissue was determined by western blotting (B) and real-time PCR (C), respectively.

inhibiting the function of the sarco/endoplasmic reticulum calcium-ATPase (SERCA) pump. The above findings indicate that *ORMDL3* may be involved in ER-associated inflammatory responses. Miller et al. found that AHR was increased in BALB/c mice overexpressing ORMDL3. These mice also exhibited changes similar to those that occur during asthmatic airway remodeling, including thickening of the bronchial smooth muscle, increased submucosal collagen deposition and increased cellulose deposition in the bronchial wall [20]. Chen et al. found that *ORMDL3* regulates airway smooth muscle hyperplasia, airway smooth muscle contraction and Ca^{2+} oscillations in asthma [21]. Our study found that *ORMDL3* was involved in the occurrence and development of airway remodeling and bronchial EMT in asthma [4]. *ORMDL3* may serve as an indicator of the severity of asthma and airway remodeling.

Asthma is related to genetic factors and is affected by a variety of environmental factors. The incidence of asthma has increased in recent years. However, the human genome does not undergo significant changes over short periods of time. The concept of asthma

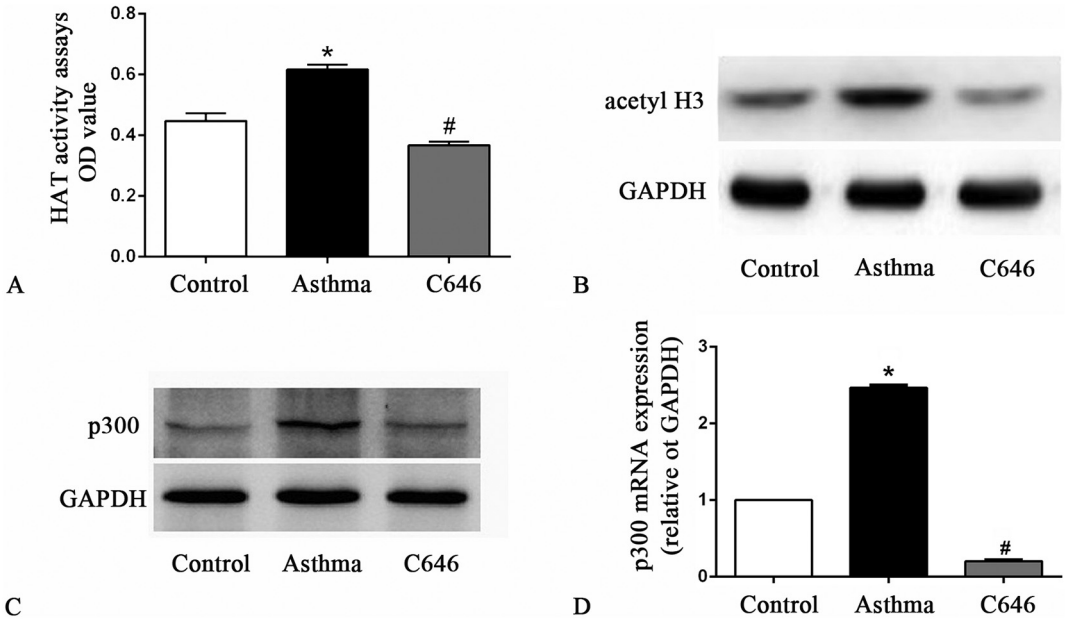

Fig. 3. Histone acetylation levels in the lung tissue of mice. HAT levels in the lung tissue of animals in the experimental groups were measured by ELISA (A) ($p < 0.01$). The expression of total aceH3 in lung tissue of the animals in different groups was measured by western blotting (B). The expression of p300 protein and mRNA in the lung tissue of animals in different groups was detected by western blotting and real-time PCR, respectively (C, D).

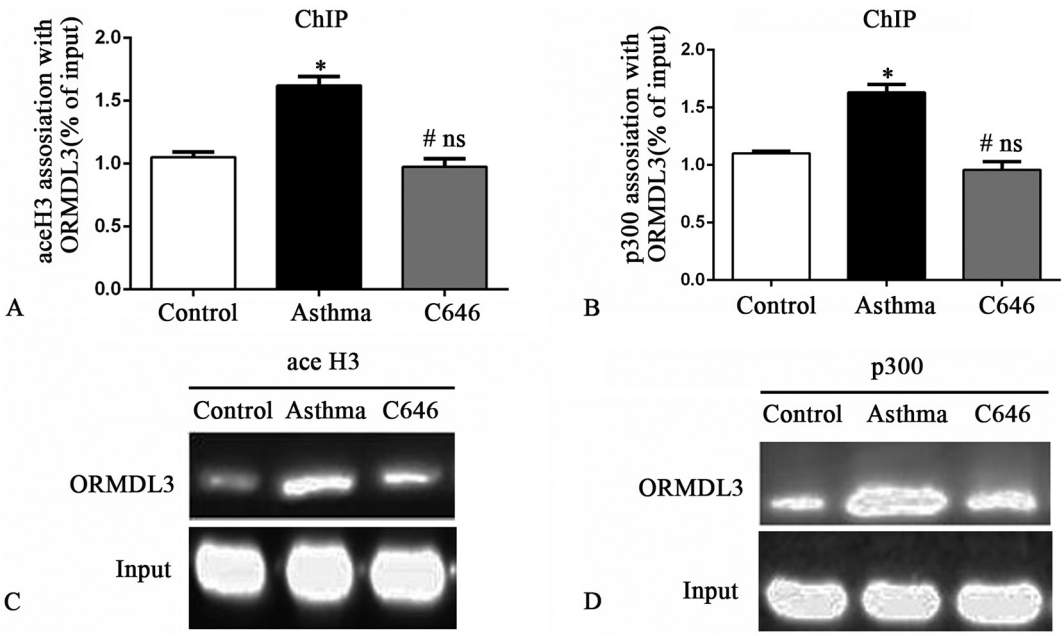

Fig. 4. The interaction between the *ORMDL3* promoter, p300 protein, and aceH3 protein. The interaction between the *ORMDL3* promoter and the p300 and aceH3 proteins was examined using real-time PCR after ChIP. Real-time PCR analysis showing the relative amount of *ORMDL3* promoter DNA bound by p300 (A) and aceH3 (C) in lung tissue of BALB/c mice in the different groups. *, Control *vs.* Asthma, $p < 0.01$; #, Asthma *vs.* C646, $p < 0.01$; ns, Control *vs.* C646, $p > 0.05$. Agarose gel electrophoretic analysis showing the relative amounts of DNA recruited by p300 (B) and aceH3 (D) in the lung tissue of BALB/c mice in different groups.

heterogeneity has been proposed [22]. Not all patients with susceptibility genes will develop asthma. Moreover, differences exist among patients carrying the same asthma susceptibility genes with respect to the age of onset, the clinical symptoms and the severity of the disease. Studies of the families of asthma patients have identified no clear pattern of inheritance. If one identical twin has asthma or other allergic diseases, the other twin does not necessarily develop the same disease [23]. Environmental factors affect the expression of genes through epigenetic modification of the genes [24]. Environmental factors include various allergens, climate, drugs, food, living conditions, social factors and early passive smoking [25]. Changes in environmental factors, especially the aggravation of air pollution in recent years, can disrupt epigenetic balance; such changes may constitute one of the reasons for the continuous increase in asthma cases in recent years [26].

Histone modification is a major mechanism of epigenetic transcriptional regulation. The acetylation and deacetylation of histones are regulated by two types of enzymes, HATs and HDACs. The two types of enzymes are functionally antagonistic. Under normal physiological conditions, HATs and HDACs are in a state of equilibrium. However, under the influence of certain physical and biochemical stimuli, the dynamic balance between HATs and HDACs is disrupted, resulting in changes in the original gene expression profile. As the result, the expression of specific molecules that affect cell proliferation, cell transformation and cell cycle regulation becomes imbalanced, eventually leading to the development of certain diseases [7].

Histone hyperacetylation has been observed in lung biopsies and in bronchial epithelial cells from patients with asthma. In addition, the ratio of HAT/HADC was shown to change with the severity of the disease [8,27]. Stefanowicz et al. found that acetylation of H3K18 was elevated in the bronchial epithelial cells of asthmatic patients [28]. The finding that hyperacetylation occurs in asthmatic lung tissues was confirmed in the present study using a BALB/c mouse model of asthma. We observed an increase in the level of p300 HAT in asthmatic lung tissues; this increase was accompanied by elevated HAT activity and increased aceH3 content. Such an increase facilitates the entry of transcription factors, thereby promoting gene transcription and increasing the release of inflammatory factors.

At present, the mechanisms underlying the regulation of *ORMDL3* gene expression remain unclear. Controlling the overexpression of *ORMDL3* may be essential for the prevention and treatment of asthma. Studies have found that p300 binding sites are present in the promoter region of the *ORMDL3* gene [11,12]; Jin's research involved the determination of the transcription initiation site of the *ORMDL3* gene, and then predicted and analyzed the promoter by bioinformatics software. The regulation of the *ORMDL3* promoter by transcription factors Ets-1, p300 and CREB was verified. The binding of Ets-1, p300 and CREB transcription factors to the promoter region of ORMDL3 was detected by ChIP. We also confirmed the combination of p300 and ORMDL3 promoters. However, whether p300 can induce the transcriptional activity of ORMDL3 needs to be further verified *in vivo* and *in vitro*. The present study demonstrated in 16HBE14o- cells and in a BALB/c mouse model of asthma that *ORMDL3* is transcriptionally regulated by p300-mediated histone acetylation. This study provides a new theoretical basis for inhibiting *ORMDL3* overexpression *in vivo* and identifies new targets for precision medical treatment of asthma. The present study first examined the effect of transfection of cells with different concentrations of p300 WT plasmid on the activity of ORMDL3. The transcription level of p300 protein reached a peak when the cells were transfected with 1 μg of the p300 plasmid; that is, the highest transfection efficiency was achieved at 1 μg. In addition, the activity of the *ORMDL3* promoter failed to increase when the amount of p300 plasmid used in the transfection was increased. Rather, the activity of the *ORMDL3* promoter increased as the expression level of p300 protein increased. *ORMDL3* promoter activity was closely related to p300 protein expression level. p300 not only affected transcription from the exogenous *ORMDL3* promoter but also played an important role in the endogenous expression of *ORMDL3* mRNA. In the present study, we transfected cells with a p300 (HAT-) plasmid and examined the luciferase activity driven by the *ORMDL3* promoter after the loss of HAT function in an attempt to confirm that p300 affects *ORMDL3* gene transcription through its HAT activity. The p300 (HAT-) plasmid was constructed by subjecting wild-type p300 to mutagenic treatment to yield the H1415A, E1423A, Y1424A, L1428S, Y1430A and H1434A

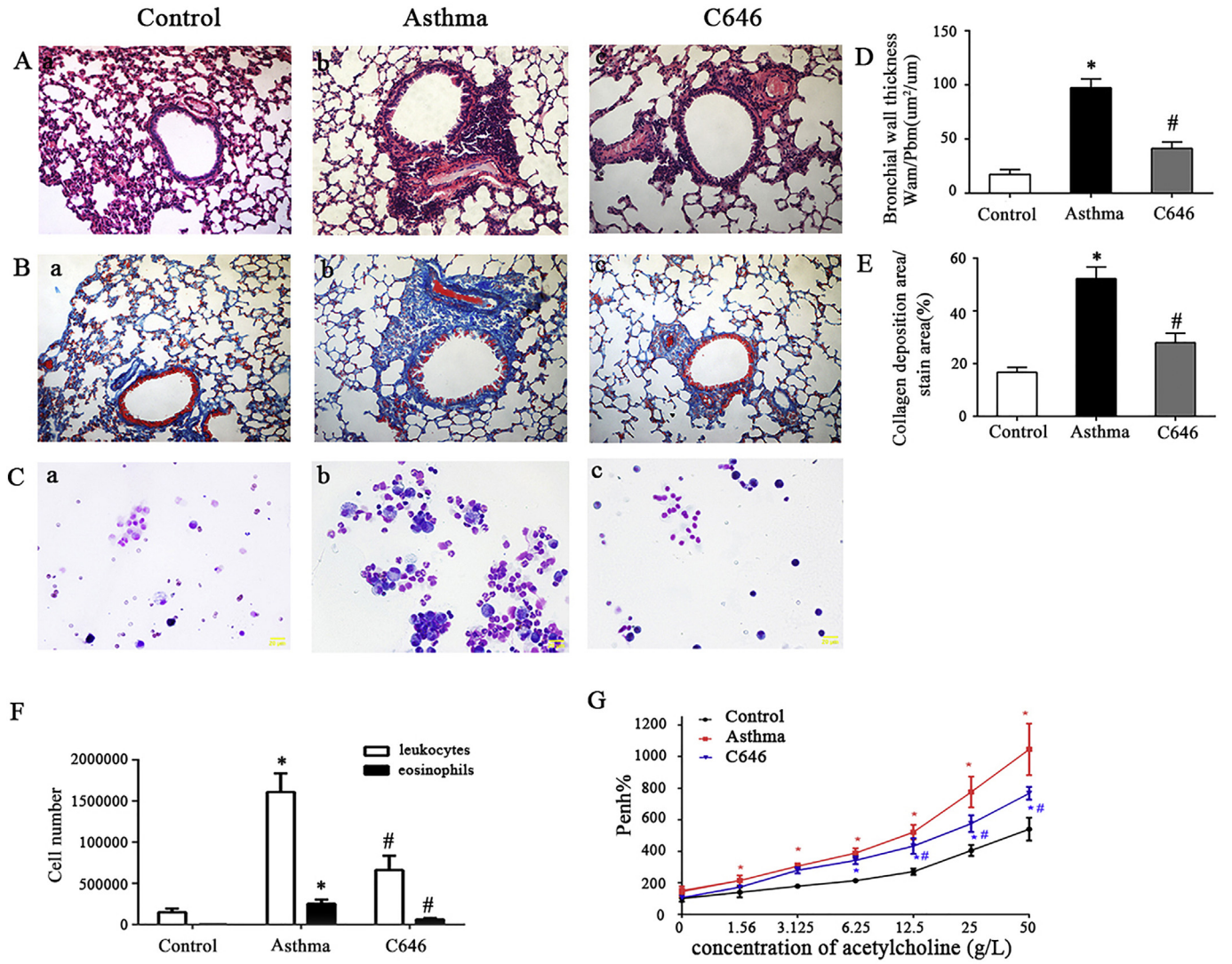

Fig. 5. The effect of C646 on airway inflammation and airway reactivity and airway remodeling in asthmatic mice. HE staining showed pathological changes in lung tissue in the control group (A a), the OVA-induced asthma group (A b), and the C646 group (A c) (magnification, ×200). Masson staining showed areas of collagen deposition in the lung tissue of the control group (B a), the asthma group (B b), and the C646 group (B c) (magnification, ×200). Total and differential cell counts of BALF were determined by Giemsa staining (C, F). Wat/Pbm, the ratio of the total bronchial wall area (Wat, μm^2) to the diameter of the basal membrane perimeter (Pbm), represents the thickness of the bronchial wall and was used to evaluate the severity of airway remodeling (D). The percentage area of collagen deposition was used to measure the severity of fibrosis in airway remodeling (E). The airways of BALB/c mice were challenged by exposure to gradually increasing concentrations of ACH (12.5–50 g/l); Penh values for the different groups were calculated (G). Compared with the control group, the Penh value increased significantly in the asthma group ($p < 0.01$). However, the Penh value of the C646 group was lower than that of the asthma group and higher than that of the control group ($p < 0.01$). *, Control *vs.* Asthma, $p < 0.01$; #, C646 *vs.* Asthma, $p < 0.01$.

mutations. In the present study, the p300 (HAT-) plasmid was transfected into 16HBE-4o cells. After transfection of the cells with the p300 (HAT-) plasmid, the activity of the *ORMDL3* promoter was not significantly different from the activity that was observed after transfection of the cells with an empty vector. In contrast, *ORMDL3* promoter activity after transfection with the p300 (HAT-) plasmid was significantly lower than the activity after transfection with the p300 WT plasmid. Transfection with the p300 (HAT-) plasmid failed to induce any change in the promoter activity or the mRNA expression of the *ORMDL3* gene. Because the deletion of the p300 HAT region did not affect *ORMDL3* expression, it can be concluded that the HAT activity of p300 is crucial for the regulation of *ORMDL3* promoter activity.

We further conducted ChIP assays to verify the relationship between *ORMDL3* and p300 in the lung tissues of BALB/c mice. The results showed that p300 and aceH3 bound to the promoter of the *ORMDL3* gene and that increased amounts of p300 and aceH3 were recruited to the *ORMDL3* promoter region in the asthma group. In addition, C646 [29] was used to inhibit histone hyperacetylation in the lung tissues of asthmatic BALB/c mice. The results showed that C646 inhibited p300 expression, reduced HAT activity and decreased aceH3 content in asthmatic mice, thereby reducing *ORMDL3* expression and improving airway remodeling and EMT. The results further demonstrated the regulatory effect of HAT on *ORMDL3* expression in an asthma model and proved that both histone acetylation and the *ORMDL3* gene are involved in the pathogenesis of asthma.

Glucocorticoids also inhibit ORMDL3 expression and are currently the most effective drugs available for controlling asthma attacks [4]. Their underlying mechanism may involve the binding of p300 to glucocorticoid receptors; such binding inhibits the HAT activity of p300 [30,31] and suppresses the expression of ORMDL3. *ORMDL3* is overexpressed in patients with refractory asthma. However, glucocorticoid receptor resistance and decreased glucocorticoid receptor activity often

occur in refractory asthma [32] and are accompanied by a severe imbalance between histone acetylation and deacetylation [33]. Therefore, it is necessary to control *ORMDL3* expression using a method that is based on its regulatory mechanism. Inhibition of the histone acetylation/deacetylation imbalance may become a new strategy for the treatment of refractory asthma.

C646 is a representative p300-selective inhibitor and is used in various studies of p300; its mechanism is mainly to inhibit the acetylase activity of p300 [34]. In this study, C646 had little effect on the expression of p300 protein, but significantly reduced the level of H3 acetylation *in vitro*. As a competitive, selective and potent small-molecule inhibitor of p300 HAT (Ki = 400 nM), C646 has activity *in vivo* and *in vitro*. C646 blocks dynamic acetylation. Compared with other acetylase inhibitors, C646 exhibits better selectivity [14]. In addition, C646 displays potent cell-penetrating ability. A number of studies have found that C646 has therapeutic effects in various disease models. The mechanism of action of C646 involves a reduction in the expression of proinflammatory cytokines that is achieved through inhibiting the HAT activity of p300 [35] and affecting the NF-κB (nuclear factor kappa-light-chain-enhancer of activated B cells) pathway [29]. C646 exerts an antitumor effect by inhibiting cell cycle progression and acts as an antiviral therapeutic agent in influenza virus-associated pneumonia [36–39]. In addition, C646 relieves chronic neuralgia caused by chronic constriction injury [40]. p300 is a central transcriptional coactivator as demonstrated by embryonic lethality when this protein is knocked out. However, inhibition of p300 overexpression to an appropriate amount can be safe. As an inhibitor of p300, C646 seldom causes toxic side effects at doses of < 5 mg/kg [36]. In the present study, individual mice were injected with 10 μg of C646 (equivalent to a dose of 0.5 mg/kg). At the above dose, C646 effectively inhibited HAT activity and reduced acetyl H3 levels. Moreover, none of the mice died as a result of the C646 injections. C646 is a drug that effectively inhibits p300 HAT and has great application value and potential. However, because there are currently insufficient data on the effects of C646, large-scale animal experiments and clinical trials are needed.

p300 is involved in the production of pro-inflammatory cytokines and regulates the transcription of pro-inflammatory genes [29,35]. p300-dependent histone H3 acetylation and C/EBPβ-regulated IKKβ expression contribute to thrombin-induced IL-8/CXCL8 expression in human lung epithelial cells [35,41], and p300 affects the NF-kB pathway and ERK pathways in lung epithelial cells [42]. The *ORMDL3* gene may be one of genes it can suppress, which can affect asthma development. Future studies should explore other mechanisms of action and pathways of p300 in asthma.

5. Conclusion

The present study demonstrated *in vitro* that p300 transfection induced the acetylation of H3 and affected *ORMDL3* expression and that the HAT activity of p300 was essential for the regulation of *ORMDL3* promoter activity. In a mouse model of asthma, *ORMDL3* expression was increased in lung tissue, and the lung tissues were in a state of histone hyperacetylation. p300 and aceH3 bound to the promoter region of the *ORMDL3* gene. In asthmatic mice, increased amounts of p300 and aceH3 were recruited to the *ORMDL3* promoter. C646, a selective acetylase inhibitor of p300, reduced *ORMDL3* expression and improved AHR and airway remodeling in asthmatic mice by inhibiting the expression of p300, reducing the activity of HAT and decreasing the level of aceH3. In summary, p300-mediated histone acetylation regulates the expression of the asthma susceptibility gene ORMDL3, thus improving the process of airway remodeling in asthma.

Ethics approval

This study was approved by the Institutional Animal Care Committee of Shengjing Hospital of China Medical University.

Consent for publication

Not applicable.

Data availability

The datasets used during the current study are available from the corresponding author on reasonable data requests.

Funding

This work was supported by 2019 National Natural Science Foundation of China (serial number: 81800029).

Authors' contributions

Cheng Qi was responsible for performing the experiments, data analysis and interpretation, and the conception of the manuscript. Shang Yunxiao was involved in the conception of the study and the manuscript. Huang Wanjie was responsible for data analysis and interpretation. Zhang Qinzhen, Li Xiang and Zhou Qianlan participated in experiments and data collection.

Declaration of competing interest

The authors declare that they have no competing interests.

Acknowledgments

Thanks to Warner Greene who gifted the plasmid to us. Thanks to American Journal Experts for language editorial assistance.

References

[1] M.F. Moffatt, M. Kabesch, L. Liang, A.L. Dixon, D. Strachan, S. Heath, M. Depner, A. von Berg, A. Bufe, E. Rietschel, et al., Genetic variants regulating ORMDL3 expression contribute to the risk of childhood asthma, Nature 448 (2007) 470–473.
[2] S.T. Weiss, B.A. Raby, A. Rogers, Asthma genetics and genomics 2009, Curr. Opin. Genet. Dev. 19 (2009) 279–282.
[3] J. Galanter, S. Choudhry, C. Eng, S. Nazario, J.R. Rodriguez-Santana, J. Casal, A. Torres-Palacios, J. Salas, R. Chapela, H.G. Watson, et al., ORMDL3 gene is associated with asthma in three ethnically diverse populations, Am. J. Respir. Crit. Care Med. 177 (2008) 1194–1200.
[4] Q. Cheng, Y. Shang, ORMDL3 may participate in the pathogenesis of bronchial epithelialmesenchymal transition in asthmatic mice with airway remodeling, Mol. Med. Rep. 17 (2018) 995–1005.
[5] I.V. Yang, D.A. Schwartz, Epigenetic mechanisms and the development of asthma, J. Allergy Clin. Immunol. 130 (2012) 1243–1255.
[6] F. Moheimani, A.C. Hsu, A.T. Reid, T. Williams, A. Kicic, S.M. Stick, P.M. Hansbro, P.A. Wark, D.A. Knight, The genetic and epigenetic landscapes of the epithelium in asthma, Respir. Res. 17 (2016) 119.
[7] T. Kouzarides, Chromatin modifications and their function, Cell 128 (2007) 693–705.
[8] P.J. Barnes, I.M. Adcock, K. Ito, Histone acetylation and deacetylation: importance in inflammatory lung diseases, Eur. Respir. J. 25 (2005) 552–563.
[9] L.P. Gunawardhana, P.G. Gibson, J.L. Simpson, H. Powell, K.J. Baines, Activity and expression of histone acetylases and deacetylases in inflammatory phenotypes of asthma, Clin. Exp. Allergy 44 (2014) 47–57.
[10] P. Bhavsar, T. Ahmad, I.M. Adcock, The role of histone deacetylases in asthma and allergic diseases, J. Allergy Clin. Immunol. 121 (2008) 580–584.
[11] L.-L. Zhuang, R. Jin, L.-H. Zhu, H.-G. Xu, Y. Li, S. Gao, J.-Y. Liu, G.-P. Zhou, Promoter characterization and role of cAMP/PKA/CREB in the basal transcription of the mouse ORMDL3 gene, PLoS One 8 (2013) e60630.
[12] R. Jin, H.G. Xu, W.X. Yuan, L.L. Zhuang, L.F. Liu, L. Jiang, L.H. Zhu, J.Y. Liu, G.P. Zhou, Mechanisms elevating ORMDL3 expression in recurrent wheeze patients: role of Ets-1, p300 and CREB, Int. J. Biochem. Cell Biol. 44 (2012) 1174–1183.
[13] S. Hasan, M.O. Hottiger, Histone acetyl transferases: a role in DNA repair and DNA replication, J. Mol. Med. (Berl) 80 (2002) 463–474.
[14] E.M. Bowers, G. Yan, C. Mukherjee, A. Orry, L. Wang, M.A. Holbert, N.T. Crump, C.A. Hazzalin, G. Liszczak, H. Yuan, et al., Virtual ligand screening of the p300/CBP histone acetyltransferase: identification of a selective small molecule inhibitor, Chem. Biol. 17 (2010) 471–482.
[15] A.L. James, J.C. Hogg, L.A. Dunn, P.D. Paré, The use of the internal perimeter to compare airway size and to calculate smooth muscle shortening, Am. Rev. Respir. Dis. 138 (1988) 136–139.

[16] E. Palmans, J.C. Kips, R.A. Pauwels, Prolonged allergen exposure induces structural airway changes in sensitized rats, Am. J. Respir. Crit. Care Med. 161 (2000) 627–635.
[17] K.W. Lee, M.E. Tory, K.J. T., Biochemical analysis of distinct activation functions in p300 that enhance transcription initiation with chromatin templates, Mol. Cell. Biol. 19 (1999) 8123–8135.
[18] C.L. Feng, M. Yajun, W.C. Greene, Acetylation of RelA at discrete sites regulates distinct nuclear functions of NF-κB, EMBO J. 21 (2002) 6539–6548.
[19] L. Hjelmqvist, M. Tuson, G. Marfany, E. Herrero, S. Balcells, R. Gonzàlez-Duarte, ORMDL proteins are a conserved new family of endoplasmic reticulum membrane proteins, Genome Biol. 3 (2002) (RESEARCH0027).
[20] M. Miller, P. Rosenthal, A. Beppu, J.L. Mueller, H.M. Hoffman, A.B. Tam, T.A. Doherty, M.D. McGeough, C.A. Pena, M. Suzukawa, et al., ORMDL3 transgenic mice have increased airway remodeling and airway responsiveness characteristic of asthma, J. Immunol. 192 (2014) 3475–3487.
[21] J. Chen, M. Miller, H. Unno, P. Rosenthal, M.J. Sanderson, D.H. Broide, Orosomucoid-like 3 (ORMDL3) upregulates airway smooth muscle proliferation, contraction, and ca(2+) oscillations in asthma, J. Allergy Clin. Immunol. 142 (1) (2018) 207–218.
[22] V. Siroux, J.R. Gonzalez, E. Bouzigon, I. Curjuric, A. Boudier, M. Imboden, J.M. Anto, I. Gut, D. Jarvis, M. Lathrop, et al., Genetic heterogeneity of asthma phenotypes identified by a clustering approach, Eur. Respir. J. 43 (2014) 439–452.
[23] S.B.R. Lawrence, I. Doull, B. Begishvili, F. Lampe, S.T. Holgate, N.E. Morton, Genetic analysis of atopy and asthma as quantitative traits and ordered polychotomies, Ann. Hum. Genet. 58 (1994) 359–368.
[24] E.J. Davidson, I.V. Yang, Role of epigenetics in the development of childhood asthma, Curr. Opin. Allergy Clin. Immunol. 18 (2018) 132–138.
[25] W. Cookson, Genetics and genomics of asthma and allergic diseases, Immunol. Rev. 190 (2002) 195–206.
[26] P.O. Brook, M.M. Perry, I.M. Adcock, A.L. Durham, Epigenome-modifying tools in asthma, Epigenomics 7 (2015) 1017–1032.
[27] A. Ferrante, B. Alaskhar Alhamwe, R. Khalaila, J. Wolf, V. von Bülow, H. Harb, F. Alhamdan, C.S. Hii, S.L. Prescott, H. Renz, H. Garn, D.P. Potaczek, Histone modifications and their role in epigenetics of atopy and allergic diseases, Allergy Asthma Clin Immunol 14 (39) (2018), https://doi.org/10.1186/s13223-018-0259-4.
[28] D. Stefanowicz, J.Y. Lee, K. Lee, F. Shaheen, H.K. Koo, S. Booth, D.A. Knight, T.L. Hackett, Elevated H3K18 acetylation in airway epithelial cells of asthmatic subjects, Respir. Res. 16 (2015) 95.
[29] T. van den Bosch, A. Boichenko, N.G.J. Leus, M.E. Ourailidou, H. Wapenaar, D. Rotili, A. Mai, A. Imhof, R. Bischoff, H.J. Haisma, F.J. Dekker, The histone acetyltransferase p300 inhibitor C646 reduces pro-inflammatory gene expression and inhibits histone deacetylases, Biochem. Pharmacol. 102 (2016) 130–140.
[30] K. Ito, E. Jazrawi, B. Cosio, P.J. Barnes, I.M. Adcock, p65-activated histone acetyltransferase activity is repressed by glucocorticoids: mifepristone fails to recruit HDAC2 to the p65-HAT complex, J. Biol. Chem. 276 (2001) 30208–30215.
[31] E. Pace, S. Di Vincenzo, M. Ferraro, L. Siena, G. Chiappara, P. Dino, P. Vitulo, A. Bertani, F. Saibene, L. Lanata, M. Gjomarkaj, Effects of carbocysteine and beclomethasone on histone acetylation/deacetylation processes in cigarette smoke exposed bronchial epithelial cells, J. Cell. Physiol. 232 (2017) 2851–2859.
[32] K. Ito, K.F. Chung, I.M. Adcock, Update on glucocorticoid action and resistance, J. Allergy Clin. Immunol. 117 (2006) 522–543.
[33] I.M. Adcock, K. Ito, P.J. Barnes, Histone deacetylation: an important mechanism in inflammatory lung diseases, COPD: J. Chron. Obstruct. Pulmon. Dis. 2 (2009) 445–455.
[34] R. Liu, Z. Zhang, H. Yang, K. Zhou, M. Geng, W. Zhou, M. Zhang, X. Huang, Y. Li, Design, synthesis, and biological evaluation of a new class of histone acetyltransferase p300 inhibitors, Eur. J. Med. Chem. 180 (2019) 171–190.
[35] F. Fang, G. Li, M. Jing, L. Xu, Z. Li, M. Li, C. Yang, Y. Liu, G. Qian, X. Hu, et al., C646 modulates inflammatory response and antibacterial activity of macrophage, Int. Immunopharmacol. 74 (2019) 105736.
[36] D. Zhao, S. Fukuyama, Y. Sakai-Tagawa, E. Takashita, J.E. Shoemaker, Y. Kawaoka, C646, a novel p300/CREB-binding protein-specific inhibitor of histone acetyltransferase, attenuates influenza A virus infection, Antimicrob. Agents Chemother. 60 (2015) 1902–1906.
[37] D.R. Warner, S.C. Smith, I.A. Smolenkova, M.M. Pisano, R.M. Greene, Inhibition of p300 histone acetyltransferase activity in palate mesenchyme cells attenuates Wnt signaling via aberrant E-cadherin expression, Exp. Cell Res. 342 (2016) 32–38.
[38] H. Sun, X. Yang, J. Zhu, T. Lv, Y. Chen, G. Chen, L. Zhong, Y. Li, X. Huang, G. Huang, J. Tian, Inhibition of p300-HAT results in a reduced histone acetylation and down-regulation of gene expression in cardiac myocytes, Life Sci. 87 (2010) 707–714.
[39] Y. Wang, K. Tu, D. Liu, L. Guo, Y. Chen, et al., p300 acetyltransferase is a cytoplasm-to-nucleus shuttle for SMAD2/3 and TAZ nuclear transport in transforming growth factor β-stimulated hepatic stellate cells, Hepatology (2019), https://doi.org/10.1002/hep.30668 (Epub ahead of print).
[40] X. Zhu, C. Huang, Q. Li, R. Chang, p300 exerts an epigenetic role in chronic neuropathic pain through its acetyltransferase activity in rats following chronic constriction injury (CCI), Mol. Pain 8 (2012) 84.
[41] Z.W. Huang, G.S. Lien, C.H. Lin, C.P. Jiang, B.C. Chen, p300 and C/EBPbeta-regulated IKKbeta expression are involved in thrombin-induced IL-8/CXCL8 expression in human lung epithelial cells, Pharmacol. Res. 121 (2017) 33–41.
[42] S. Xu, Q. Liu, H. Yang, X. Sun, Downregulation of p300 alleviates LPS-induced inflammatory injuries through regulation of RhoA/ROCK/NF-κB pathways in A549 cells, Biomed. Pharmacother. 97 (2018) 369–374.